LCLS-II Technical Note

Studies of Misalignment Tolerances for SC Linac of LCLS-II

LCLS-II TN-14-03

3/21/2014

Arun Saini, N. Solyak, V. Yakovlev

1 Introduction

Linac Coherent Light Source (LSLS) –II is a proposed fourth generation x-ray light source facility. It is based on 4 GeV superconducting radio frequency (SCRF) linear accelerator (linac) that would operate in continuous wave (CW) regime. One of the primary accelerator design and operation objectives for LCLS-II linac would be the preservation of beam emittances. Various sources of emittance dilution in linac include dispersion originating from misalignment of quadrupoles and BPMs, pitched cavities and cryomodules (girders), wake fields generated from cavity offsets and coupling between the transverse planes due to rotated quads (or skew) etc. In order to preserve beam emittance along the linac, stringent tolerances on alignment of beamline elements are applied. In this work, we present studies performed to understand linac behavior in presence of various misalignments. In addition, beneficial effect of orbit correction using one to one steering algorithm on emittance dilultion is also discussed.

2 SCRF Linac

SCRF linac is composed of five superconducting sections that are named as L0, L1, HL, L2, and L3. Configuration of each section is summarized in table 1. HL section consists of third harmonic i.e. 3.9 GHz cavities [1] which are used to linearize longitudinal beam profile in order to suppress non-linear effects in bunch compressor. All other sections are composed of 1.3 GHz cavities [2-3]. L2 and L3 are major sections and therefore determine alignment tolerance of components in linac. Thus, this work is mainly focused on L2 and L3 which are studied independently.

Table 1: Configuration of each section in SCRF Linac.

Linac Section	*Number of Cryomodules*	*Number of Cavities per Cryomodules*	*Accelerating Grad. (MV/m)*	*Sync. Phase (degree)*	*Energy Range (MeV)*
L0	1	8	14.78	*	0.75 -95
L1	2	8	13.43	-21.0	95 - 303
HL	3	4	13.246	-165.0	303-250
L2	12	8	14.515	-21.0	250-1600
L3	20	8	14.455	0.0	1600-4000

* Phases in each cavity of L0 are 3.4, -15.2, 0, 0, 0, 15,15, 0

Betatron functions (β_x, β_y) for baseline design of L2 and L3 are shown in Fig 1. Phase advance per period in L2 and L3 are about 30^0 and 15^0 respectively.

3 Tolerances Studies

The main obstacle to emittance preservation in linac is alignment of quadrupoles and RF cavities with respect to survey line. When a bunch asses through a misaligned quadrupole, particles within bunch start to make betatron oscillations with different betatron wavelengths due to finite energy spread among the particles in a bunch. As a result, the particles with low and high energy no longer oscillate coherently with each other that result in emittance growth.

Horizontal or vertical offset of cavities result in short range wakefields that act back on beam and cause transverse deflection of trailing particles in the bunch. Due to uncorrelated misalignments, the kicks from large number of cavities will tend to cancel each other. However, due to finite number of cavities, kick cancellation is usually imperfect and it results in degradation in beam quality and therefore, emittance growth.

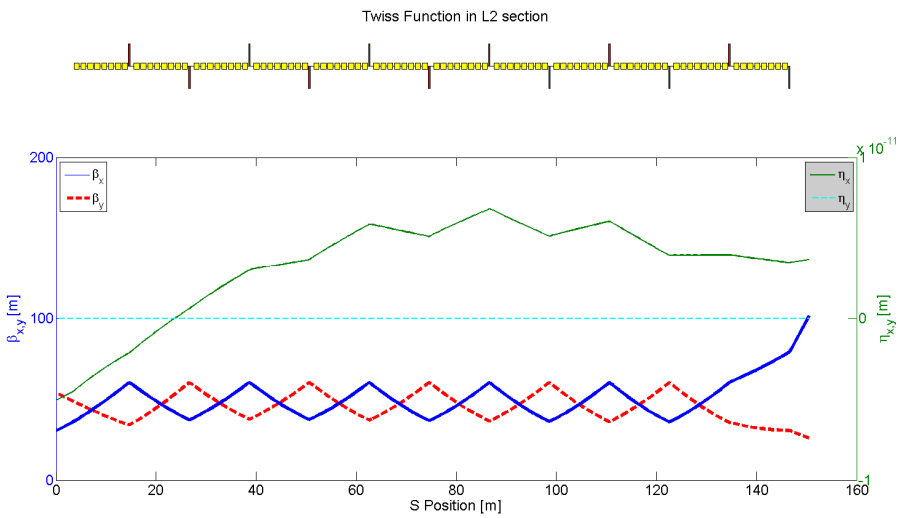

(a)

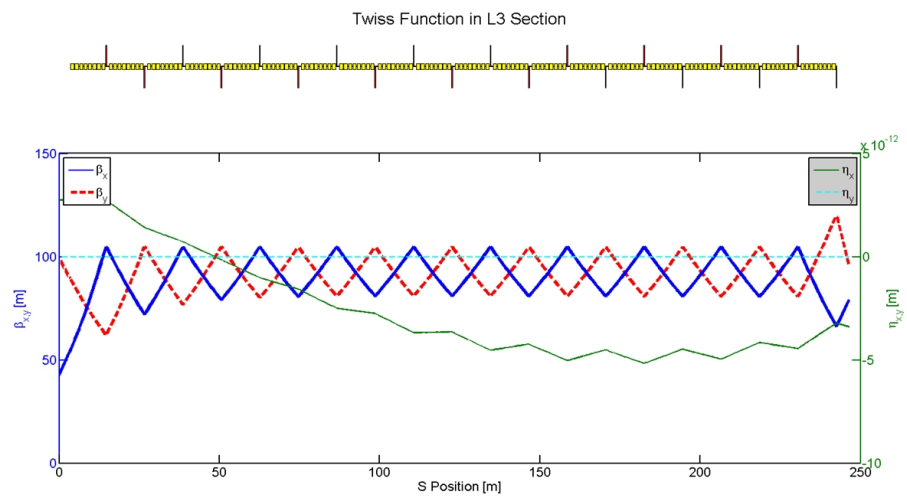

(b)

FIG. 1: Betatron function along L2 (a) and L3 (b) section.

Sometime beamline elements are misaligned in such a way that they have net slope with respect to cryomodule axis in *x-z* or *y-z* plane. However, longitudinal center of element is properly aligned. This kind of misalignment is referred as tilt or pitched. It is primarily concerned for RF cavities where tilting causes coupling of longitudinal field into transverse planes. Thus, there is a resulting deflection experienced by particles passing through the cavity. Furthermore, head and tail arrive at different time and therefore experience different transverse kick from time varying field. Emittance growth due to tilted cavities might be significant at low energy part of linac where bunch is relatively long and cavities are not operated at crest. Figure 2 summarizes possible cavity alignment in beam line. Emittance dilution due to wake kick in tilted cavities is small. Wake kicks in the upstream half of cavity is cancelled by wake kicks in the downstream part. However, cancellation is not perfect as energy also changes along the RF cavity but its effect is minimal.

Misalignment of cryomodule (also called girder sometime in this note) with respect to survey line may also occur in real beam line and it introduces sort of correlated misalignment of elements in cryomodule. Thus, it also results in emittance dilution.

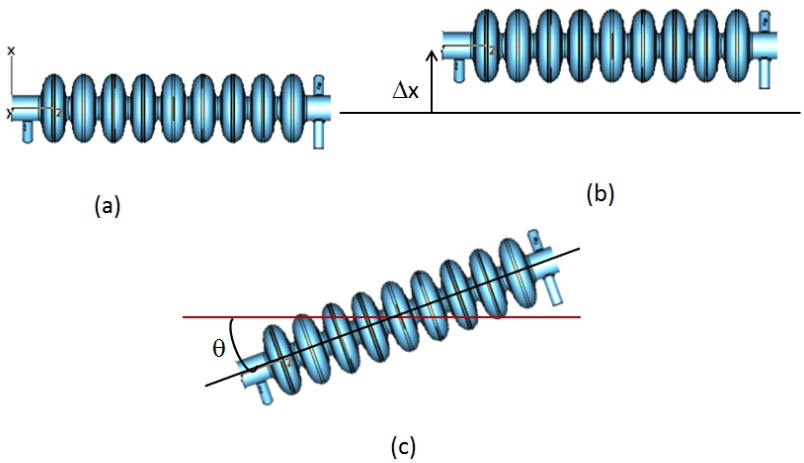

FIG. 2: Position of RF cavity in beamline: (a) perfectly aligned, (b) offset in horizontal direction, (c) tilted or pitched cavity.

On the basis of experience gained from experimental measurements and studies performed for proposed SC linear accelerator facilities such as XFEL, ILC, TESLA etc., a set of alignment requirement of beamline elements in SC linac of LCLS-11 facility is generated and specified in Table 2.

Table 2: Nominal RMS misalignment tolerances for the LCLS-II cryomodules.

Injection transverse jitter	***1 sigma RMS errors***	***Units***
Cavity misalignments wrt. CM	0.5	mm
Cavity tilts	0.5	mrad
Quadrupoles misalignments wrt. CM	0.5	mm
BPM misalignments wrt. CM	0.5	mm
Cryomodule misaligments	0.5	mm
Cryomodule tilt	0.05	mrad
BPM resolution	0.01	mm

3.1 L2 section

L2 section is used to accelerate the beam from kinetic energy of 0.25 GeV to 1.6 GeV. It is composed of 12 cryomodules and each cryomodule consists of eight 1.3 GHz cavities and one quadrupole at the end. Misalignment studies are performed for lattice v1.2 [4] using beam dynamics code LUCRETIA [5]. Simulation is performed for 300 pC bunch charge with initial normalized rms emittance of 0.35 and 0.36 in horizontal and vertical plane respectively. RMS bunch length and relative energy spread at the beginning of L2 section are 0.27 mm and 1.33 % respectively. The misalignment specified in table 2 is applied in vertical plane and 50 machines (seeds) are studied for given set of misalignment errors.

Figure 3(a) shows vertical beam trajectories for 50 machines simulated for L2 section in presence of all nominal misalignments. It can be seen that beam might get shifted up to 6 mm. Figure 3(b) shows normalized rms vertical emittance growth along the L2 section. It can also be noticed from figure 3(b) that some of seeds result in emittance growth ($\Delta\varepsilon_y$) of 0.10 mm mrad. However, 90 % emittance growth as shown in figure 4 is about 0.05 mm mrad.

In order to correct beam trajectory and hence minimizing emittance growth, one to one steering algorithm is applied. Settings in correctors are chosen in such a way that beam is steered to center of all

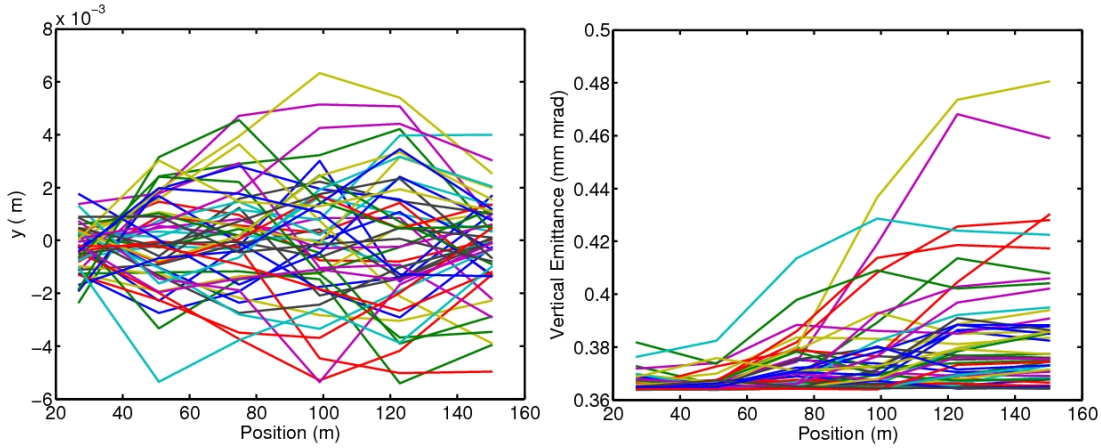

(a) (b)

FIG. 3: (a) Beam vertical trajectories and (b) normalized rms vertical emittances for 50 seeds of applying all nominal misalignments to the L2 section.

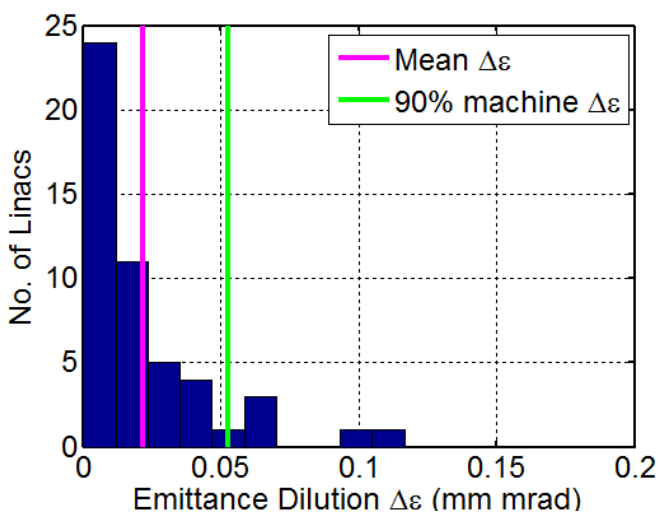

FIG. 4: Resulting 90% emittance growth for 50 seeds of applying all nominal misalignments to L2 section.

beam position monitors (BPMs). It is one of simplest still effective tuning algorithm. However, performance of one to one steering depends on alignment of BPMs.

There is one vertical corrector and BPM associated with each vertical focusing quad (similarly one horizontal corrector and BPM with horizontal focusing quad) in L2 section. Figure 5 shows beam trajectories of 50 seeds of all nominal errors before (blue) and after (green) applying 1-1 corrections. It can be seen that beam golden trajectories that include beam vertical position and BPMs offset (shown in green) is corrected within 2 mm offset. Evolution of emittance growth for corresponding seeds is shown in figure 6. It can be observe from figure 6(a) that emittance dilution is compensated significantly after applying one to one corrections. Relative rms emittance growth ($\Delta\varepsilon_y/\varepsilon_y^{initial}$) at the end of section are about 7 % and 1 % before and after 1-1 correction respectively. Figure 6(b) shows relative rms emittance growth before (blue) and after correction (green). Different scenarios of element misalignments are studied. Projected emittance dilutions in L2 section for different cases are summarized in table 3 and corresponding relative rms emittance dilutions are shown in figure 7.

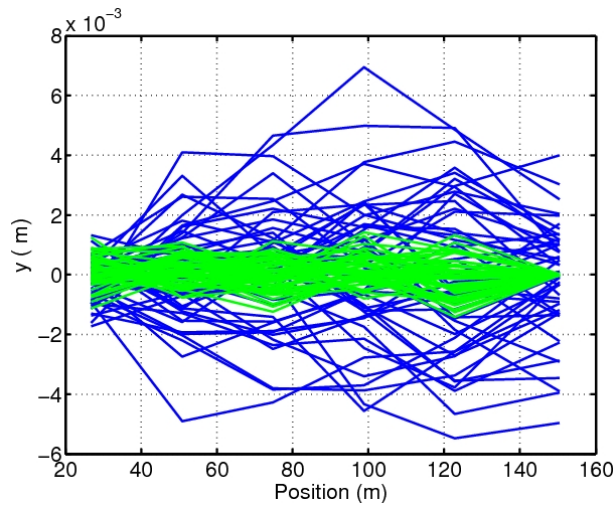

FIG 5: Beam trajectories for 50 seeds: without correction in blue and after 1-1 corrections in green (golden trajectories that includes y+ BPM offset)

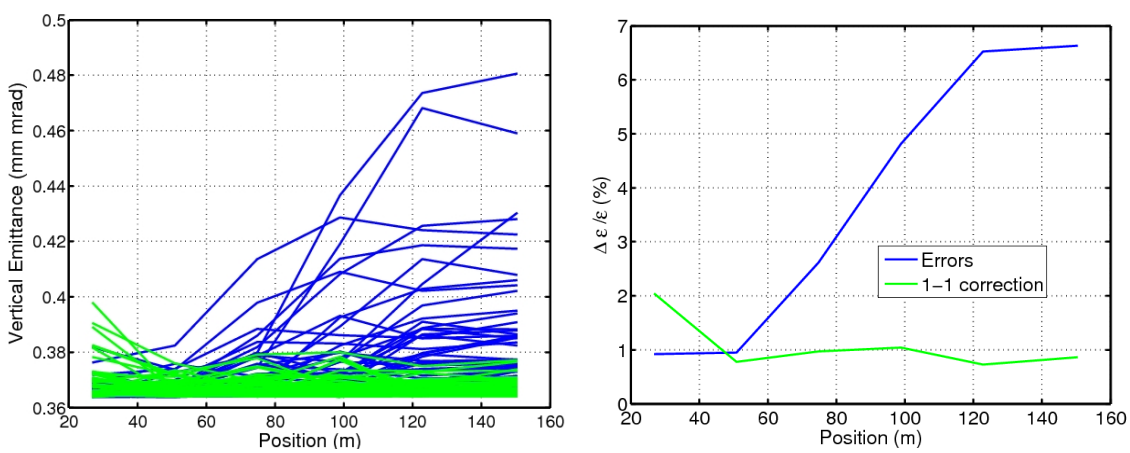

(a) (b)

FIG 6: Emittance evolution before (blue) and after (green) 1-1 correction along L2 section: (a) Normalized rms vertical emittance and (b) relative rms emittance growth.

Table 3: Projected emittance dilution in different cases of element misalignments in L2 section.

	Offset	Tilt	$\Delta\varepsilon_y/\varepsilon_y^{initial}$	90 % machine Emittance	$\Delta\varepsilon_y/\varepsilon_y^{initial}$ (1-1 correction)
Units	mm	mrad	%	mm mrad	%
Cavity	0.5	-	0.02	0.0001	0.004
Cavity	-	0.5	2.3	0.017	0.11
Quads+BPMs	0.5	-	2.0	0.018	0.40
Girder	0.5	-	2.6	0.016	0.2
Girder	-	0.05	1.4	0.01	0.12
All	0.5	0.5+ 0.05*	6.6	0.053	0.9

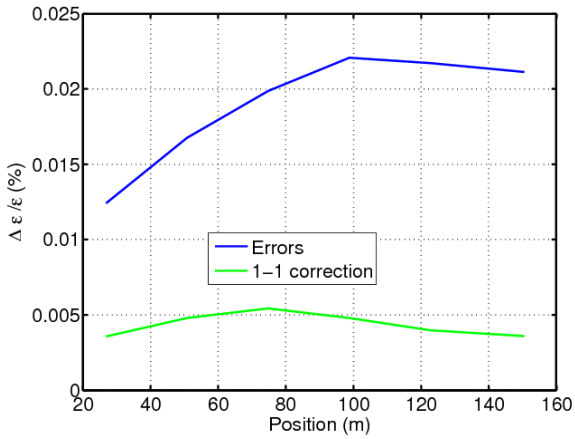

(a)

Cavity Offset

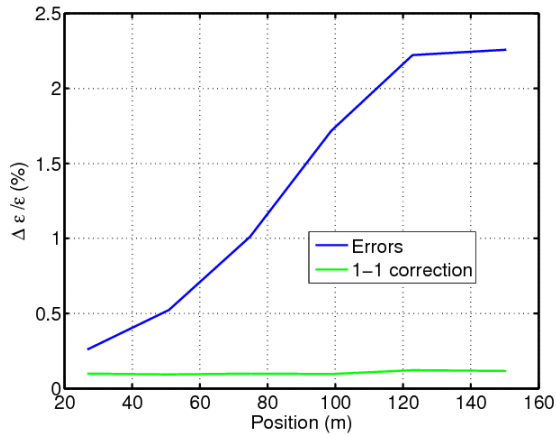

(b)

Cavity Tilt

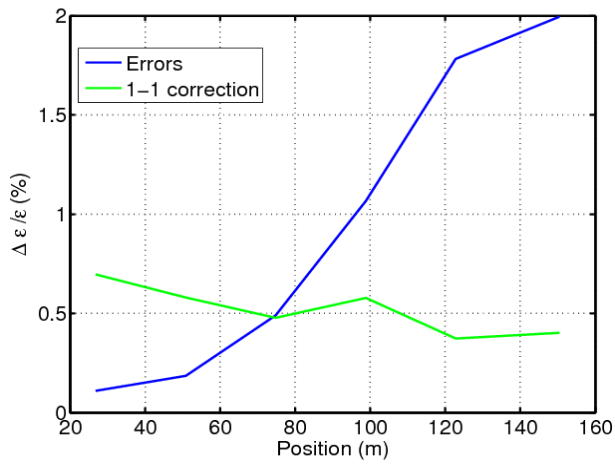

(c)

Quadrupoles and BPMs Cavity Offset

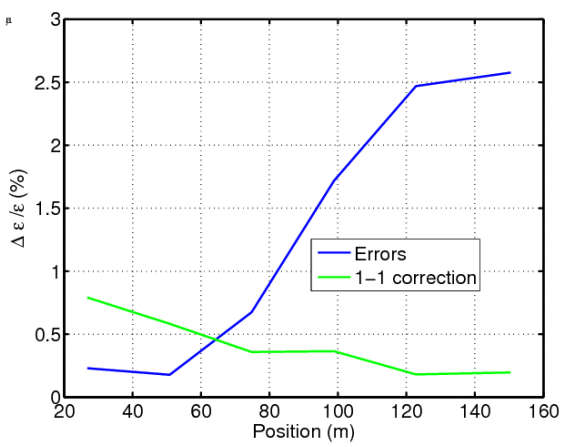

(d)

Girder Offset

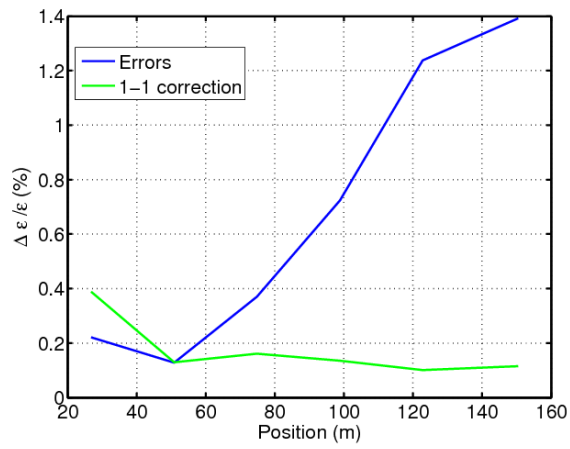

(e)

Girder Tilt

FIG 7: Projected emittance dilution for different cases of element misalignments in L2 section.

3.2 L3 Section

L3 section will be used to accelerate the beam from energy of 1.6 GeV to 4 GeV. This section is composed of 20 cryomodules of 1.3 GHz cavities. Similar studies have been performed to analyze misalignment tolerances for L3 section.

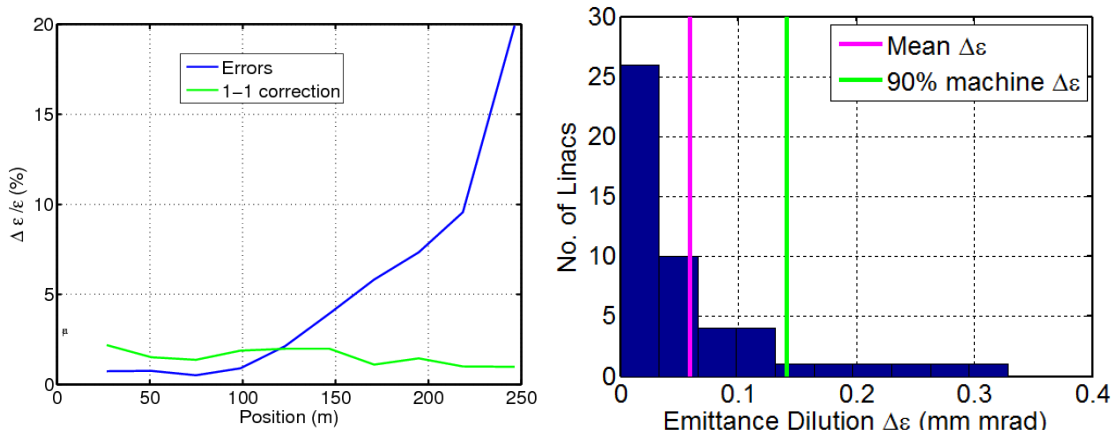

(a) (b)

FIG 8: (a) Relative rms emittance dilution before (blue) and after (green) applying 1-1 steering correction and (b) 90 % machine acceptance for 50 seeds of all nominal misalignments in L3 section.

Evolution of emittance in L3 section for 50 seed of all nominal misalignments is shown in figure 8. It can be noticed that after applying one to one correction, emittance dilution is reduced significantly from ~20 % to 1% that helps to restore beam quality along the section. Emittance dilution for 90% of machine (no correction) is shown in figure 8(b).

Studies are performed to analyze different scenarios of element misalignments in L3 section. Results are summarized in table 4 and corresponding emittance evolution is shown in figure 9.

Table 4: Projected emittance dilution in different cases of element misalignments in L3 section.

	Offset	Tilt	$\Delta\varepsilon_y/\varepsilon_y^{initial}$	90 % machine Emittance	$\Delta\varepsilon_y/\varepsilon_y^{initial}$ (1-1 correction)
Units	mm	mrad	%	mm mrad	%
Cavity	0.5	-	0.006	0.00004	0.002
Cavity	-	0.5	1.3	0.011	0.01
Quads+BPMs	0.5	-	4.4	0.040	0.44
Girder	0.5	-	9.55	0.090	0.55
Girder	-	0.05	3.75	0.019	0.14
All	0.5	0.5+ 0.05*	19.9	0.14	0.98

In order to understand threshold and margin of tolerances with nominal misalignment, all misalignments are doubled in magnitude. Results are summarized for L2 and L3 section in table 5.

Table 5: Projected emittance dilution in L2 and L3 with twice of magnitude of all misalignments.

	$\Delta\varepsilon_y/\varepsilon_y^{initial}$ (%)	90 % machine Emittance	$\Delta\varepsilon_y/\varepsilon_y^{initial}$ (1-1 correction) (%)
L2	21.6	0.192	3.24
L3	54.1	0.42	3.51

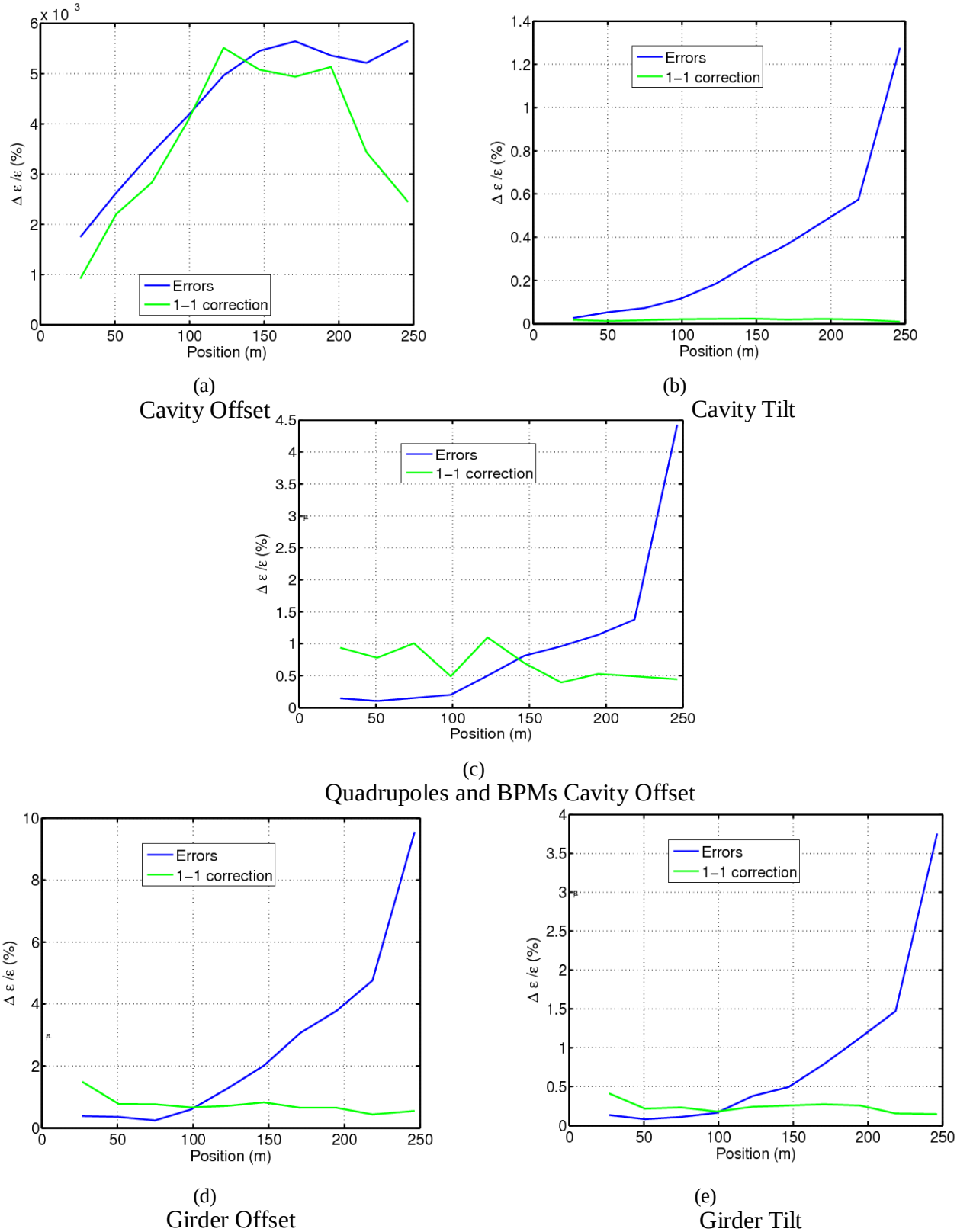

FIG 9: Projected emittance dilution for different cases of element misalignments in L3 section.

It can be noticed that emittance dilution is limited to ~ 3.5 % after 1-1 steering.

3.3 Studies for new nominal misalignments

Table 6: New Nominal RMS misalignment tolerances for the LCLS-II cryomodules [6].

Error Source	RMS error	unit
Cavity X,Y misalignments wrt. CM	0.5	mm
Quadrupole X,Y misalignments wrt. CM	0.5	mm
BPM X,Y misalignments wrt. CM	0.5	mm
Cryomodule X,Y misalignments wrt. Linac	0.3	mm
Cavity Z misalignments wrt. CM	2	mm
Quadrupole Z misalignments wrt. CM	2	mm
BPM Z misalignments wrt. CM	2	mm
Cryomodule Z misalignments wrt. Linac	2	mm
Cavity tilt misalignments	0.5	mrad
Quadrupole tilt misalignments	3	mrad
BPM tilt misalignments	3	mrad
Cryomodule tilt misalignments	0.05	mrad
Cavity roll misalignments	10	mrad
Quadrupole roll misalignments	3	mrad
BPM roll misalignments	3	mrad
Cryomodule roll	2	mrad

Studies are performed for new lattice (March 2014) with new set of nominal misalignments that are summarized in table 6 [6]. An Initial offset of beam results in coherent betatron oscillations along the linac. Thus, this effect is also included in estimation of emittance dilution.

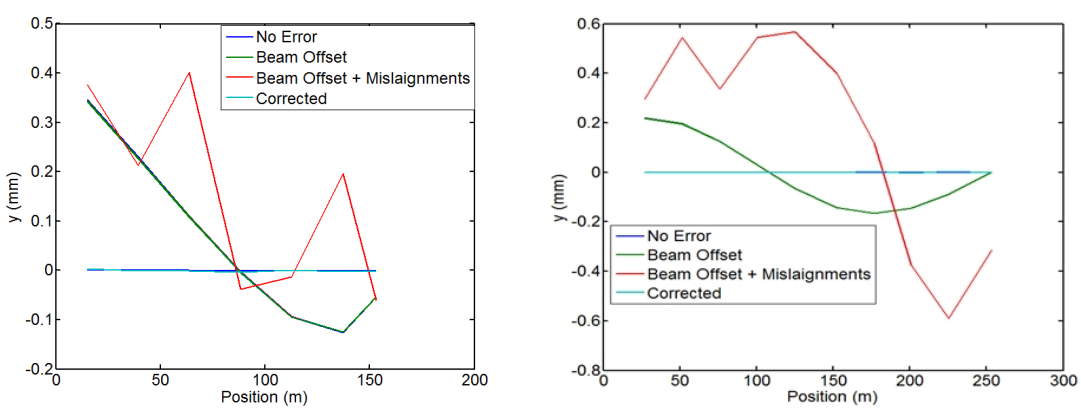

(a) (b)

FIG 10: Beam trajectory along (a) L2 section and (b) L3 section.

Figure 10 shows beam trajectory along L2 and L3 for different cases. It can be observed that trajectory is corrected after applying 1-1 correction.

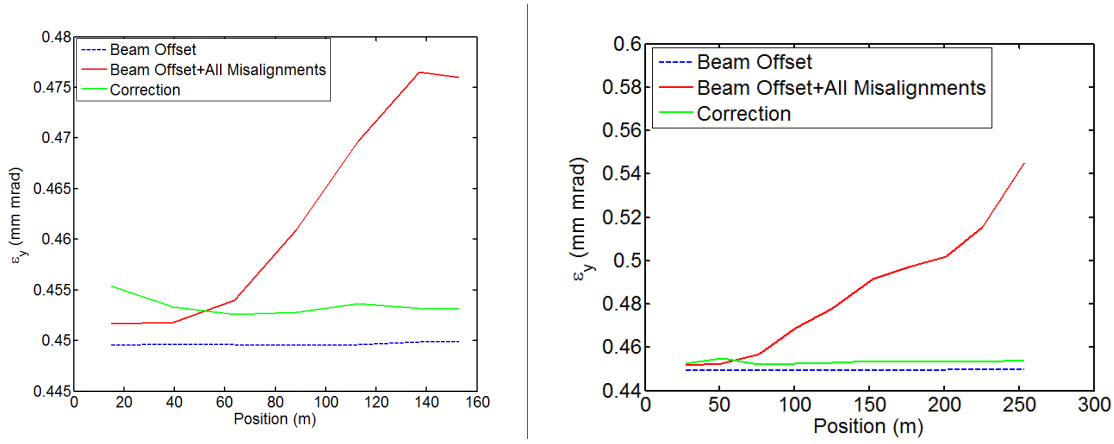

(a) (b)

FIG : 11 Project emittance growth along (a) L2 and (b) L3 sections.

Figure 11 shows emittance growth in L2 (left) and L3 (right) section and results are summarized in table 7. . It should be noted that initial beam emittance is 0.45 mm mrad (instead of 0.35 used in earlier studies)

Table 7: Projected emittance dilution in L2 and L3 with new set of misalignments.

	$\Delta\varepsilon_y/\varepsilon_y^{\text{initial}}$ (%)	90 % machine Emittance	$\Delta\varepsilon_y/\varepsilon_y^{\text{initial}}$ (1-1 correction) (%)
L2	6.7	0.059	1.1
L3	18.4	0.198	1.0

4 Conclusion

Studies are performed to analyze alignment tolerances of beamline elements in L2 and L3 section. Impact of cavity misalignments particularly cavity pitch is stronger at low energy (L2). Girder misalignment results in a sort of correlated misalignment among elements of a girder. Thus, girder misalignments are major source of emittance dilution. Studies show that 1-1 steering correction is quite effective in order to compensate emittance dilution. It is observed that emittance dilution in linac (L2 & L3) is limited to ~ *1%* after applying 1-1 correction.

It is also demonstrated that lattice (L2 & L3) is robust enough to deal with misalignments which are twice in magnitude than nominal misalignments. Emittance dilution after applying 1-1 steering in this case is less than *4 %* for L2 and L3 section.

References:

[1] "Development of the Superconducting 3.9 GHz Accelerating cavity at Fermilab," N. Solyak et al. http://lss.fnal.gov/archive/2005/conf/fermilab-conf-05-121-td.pdf
[2] B. Aune et al, Phys. Rev. ST Accel. Beams 3, 092001 (2000).
[3] ILC reference design report, volume 3- Accelerator, (2007) http://www.linearcollider.org/about/Publications/Reference-Design-Report
[4] http://www.slac.stanford.edu/cgi-wrap/cvsweb/optics/etc/lattice/lcls2/mad/?cvsroot=LCLS
[5] http://www.slac.stanford.edu/accel/ilc/codes/Lucretia/

[6] "SCRF 1.3 GHz Cryomodule," Physics Requirements Document (PRD), LCLSII-4.1-PR-0146-R0. https://docs.slac.stanford.edu/sites/pub/Publications/SCRF_1.3_GHz_Cryomodule.pdf

Appendix

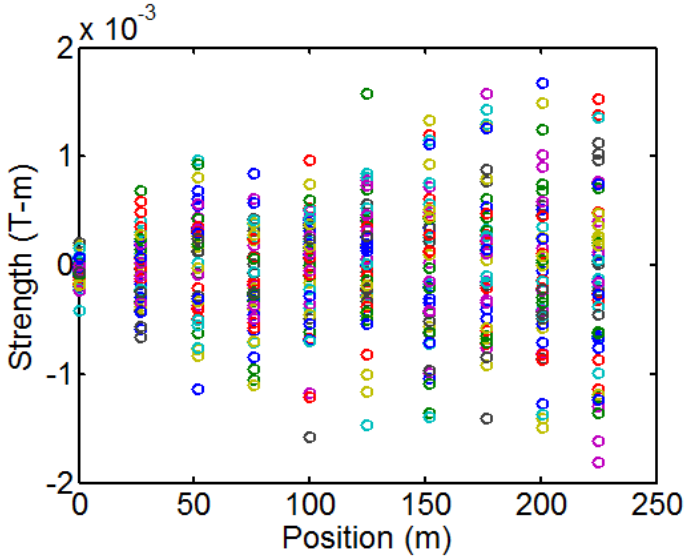

FIG 12: Distribution of fields in correctors for all 50 seeds with nominal misalignments (corresponding to Table 6) in L3 section.

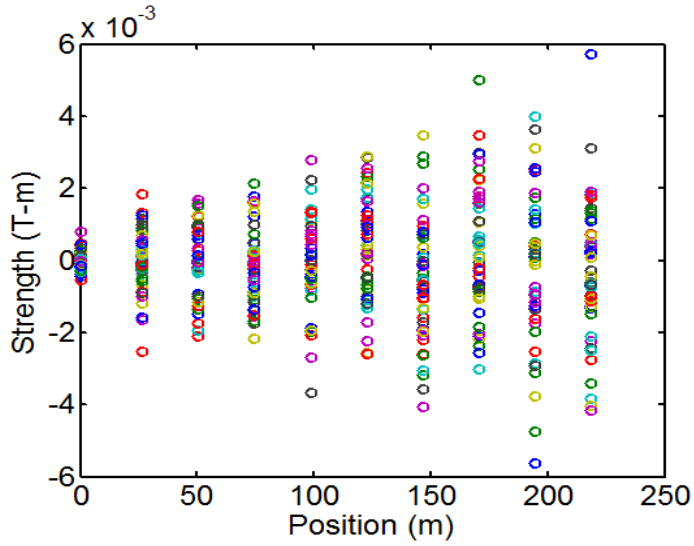

FIG 13: Distribution of fields in correctors for all 50 seeds with misalignments twice in magnitude than nominal (twice of table 2) in L3 section.